



**HAL**  
open science

## The physics of cell-size regulation across timescales

Clotilde Cadart, Larisa Venkova, Pierre Recho, Marco Cosentino  
Lagomarsino, Matthieu Piel

► **To cite this version:**

Clotilde Cadart, Larisa Venkova, Pierre Recho, Marco Cosentino Lagomarsino, Matthieu Piel.  
The physics of cell-size regulation across timescales. *Nature Physics*, 2019, 15 (10), pp.993-1004.  
10.1038/s41567-019-0629-y . hal-02359349

**HAL Id: hal-02359349**

**<https://hal.science/hal-02359349>**

Submitted on 4 Jan 2021

**HAL** is a multi-disciplinary open access archive for the deposit and dissemination of scientific research documents, whether they are published or not. The documents may come from teaching and research institutions in France or abroad, or from public or private research centers.

L'archive ouverte pluridisciplinaire **HAL**, est destinée au dépôt et à la diffusion de documents scientifiques de niveau recherche, publiés ou non, émanant des établissements d'enseignement et de recherche français ou étrangers, des laboratoires publics ou privés.

**Title:** The physics of cell-size regulation across timescales

**Authors:** Clotilde Cadart<sup>1,2\*</sup>, Larisa Venkova<sup>1,2\*</sup>, Pierre Recho<sup>3§</sup>, Marco Cosentino Lagomarsino<sup>4,5,6§</sup>,  
Matthieu Piel<sup>1,2§</sup>

1 Institut Curie, PSL Research University, CNRS, UMR 144, F-75005, Paris, France

2 Institut Pierre-Gilles de Gennes, PSL Research University, F-75005, Paris, France

3 LIPhy, CNRS-UMR 5588, Université Grenoble Alpes, F-38000 Grenoble, France

4 Physics Department, University of Milan, 20133 Milan, Italy

5 CNRS, UMR 7238 Computational and Quantitative Biology, Paris, France

6 FIRG Institute of Molecular Oncology (IFOM), Milan, Italy

§ Correspondence should be sent to: pierre.recho@univ-grenoble-alpes.fr, marco.cosentino-lagomarsino@ifom.eu and matthieu.piel@curie.fr

\* these authors contributed equally to the work

**Abstract:**

The size of a cell is determined by a combination of synthesis, self-assembly, incoming matter and the balance of mechanical forces. Such processes operate at the single-cell level, but they are deeply interconnected with cell-cycle progression, resulting in a stable average cell size at the population level. Here, we examine this phenomenon by reviewing the physics of growth processes that operate at vastly different timescales, but result in the controlled production of daughter cells that are close copies of their mothers. We first review the regulatory mechanisms of size at short timescales, focusing on the contribution of fundamental physical forces. We then discuss the multiple relevant regulation processes operating on the timescale of the cell cycle. Finally, we look at how these processes interact: one of the most important challenges to date involves bridging the gap between timescales, connecting the physics of cell growth and the biology of cell-cycle progression.

Main text (no heading):

Size may seem to be the most trivial aspect of cell morphology, but the mechanisms regulating cell size have been studied less than cell polarity or shape. One view holds that growth processes operating on different timescales work together to control cell size. Though appealing, this approach is hampered by the fact that different timescales are typically studied by different scientific communities: cell-size fluctuations occurring on short timescales, such as those related to osmosis or cell spreading, are primarily considered by physicists studying cell mechanics, whereas the long timescale orchestration of cell growth and division is usually addressed from a purely biological standpoint. Here we unify these approaches in a review of cell-size control across different timescales.

Within this framework, a cell-size parameter constitutes the sum of any quantity over the domain enclosed in the cell membrane. This includes mass, volume, surface area, but also many other quantities — each parameter being a proxy for a different biological, chemical or physical process. For example, the volume defines the spatial or steric role of a cell in its environment, whereas dry mass represents the sum of the materials (including proteins and other biomolecules) needed for the cell to remain operational, and cell surface defines an effective area of exchange with the exterior. All these parameters are subject to specific ‘homeostatic’ regulation, meaning a feedback loop that controls the quantity at a certain set point. Such controls operate at different scales because size is regulated both at the single cell and the cell population level over different timescales.

Size parameters can fluctuate in individual cells or globally shift within a population, and these changes are coupled together to achieve global cell-size homeostasis. For example, the ratio of dry mass to volume defines a cell density. This quantity is related to intracellular concentrations, hence to the rates of chemical reactions occurring in the cell<sup>1,2</sup>. Similarly, mechanisms ensuring surface-tension homeostasis<sup>3</sup> can couple volume and surface area<sup>4,5</sup>. These examples hint at how global size homeostasis could be the result of a small number of intrinsic and extrinsic parameters driving global growth, coupled by both biological and physical effects.

Such couplings could also ensure the homeostasis of cell-size distribution in a population by modulating growth rates and the duration of cell-division cycles. These processes are probably coupled to biological pathways, and show how a pathway could directly associate with cell-size parameters without a complex dedicated sensing circuit. These and other effects likely connect short-timescale size fluctuations to longer-term growth, but our understanding of these links is still limited. Indeed, as we will detail in this review, the least understood problems lie at intermediate timescales, where physical processes affecting size parameters are coupled to biological feedback.

The aim of this review is thus to bridge the gap between the short-timescale homeostatic mechanisms setting the volume, mass and surface area of the cell by regulating processes like water entry, membrane trafficking and protein synthesis, and the long-timescale size homeostasis set by growth and division. We start with short timescales (seconds and minutes), on which physical and regulatory processes can modulate surface area and volume at fixed cell content, for example by osmoregulation and cytoskeletal organization. We then address how on the timescales of a cell-division cycle, in a population of proliferating cells, cell size results from the interplay of growth and cell-cycle timing. Both areas have been the subject of intense debate in recent years, but we believe that the discourse suffers from a lack of connection between these two kinds of process. In the third part of the review we address open problems concerning the fact that growth–division and volume–surface modulation work on overlapping timescales, so their coupling may be important in setting individual cell sizes.

For sake of brevity, two layers of complexity are omitted from our discussion. First, it is possible that cell-size homeostasis also results from mechanisms acting at the level of subcellular compartments, which would themselves scale to global cell-size parameters and serve as internal ‘rulers’<sup>6</sup>. One example is the nucleus, whose size has been shown to be proportional to cell size via the titration of a surface-area-to-volume sensor<sup>7</sup>. Although this is an interesting hypothesis, the current lack of experimental evidence for such phenomena prompted us to exclude discussion of the regulation of the size of cellular organelles. Second, complexity of behaviour in size parameters can emerge from multicellularity or from factors that produce feedback at the level of the cell population, such as quorum sensing in populations of unicellular organisms. Several global factors are also regulated at the tissue and organism level. These include chemical cues, including hormones and morphogens, which are well documented in *Drosophila*<sup>8</sup>, as well as physical factors, such as mechanical stress and electric fields<sup>9</sup>. We thus restrict this review to cell-autonomous mechanisms acting at the single-cell level, excluding higher levels of homeostasis.

### **Cell size homeostasis at short timescales**

We begin by reviewing the mechanisms by which cells adapt their volume on short (seconds) to intermediate (minutes) timescales. Most of this knowledge comes from the study of the response to osmotic shocks, because this is the easiest experimental way to impose rapid volume changes.

#### *The physical basis of cell-volume regulation at short timescales*

Solid cell components, such as cell organelles or the cytoskeleton, only occupy about 30% of the total cell volume, even when the associated water is taken into account<sup>10</sup>. Hence, the most basic problem of cell-size regulation is to understand how water flows in and out of cells. This problem can be addressed experimentally by considering how cells control their volume robustly when faced with rapid external perturbations. For example, bovine aortic endothelial cells can react to extreme hypotonic<sup>11</sup> and hypertonic environments and survive for hours. We review and explain below how such regulation is accomplished for different cell types. The physical principles of mass and force conservation, as well as near-equilibrium thermodynamics, offer generic guidelines to understand how this water flux is driven and how it can be biologically regulated.

Water mobility in and out of the cell relies on the permeation of water through the plasma membrane, which can be regulated by aquaporin channels (AQP)<sup>12</sup>. These channels are permeable to water, glycerol and some small molecules, but not to ions. Assuming that they do not consume ATP to work (See **Box 1** and ref. <sup>13</sup>), the incoming water flux  $J_w$  is proportional to the difference of two chemo-mechanical driving forces: the osmotic pressure,  $\Pi$  and the hydrostatic pressure,  $p$

$$J_w = L_p(\Delta p - \Delta\Pi) \quad (1)$$

where  $\Delta$  denotes the difference of a quantity between the cell exterior and interior. The factor of proportionality  $L_p$  is the filtration coefficient of the membrane<sup>14</sup>, which depends on the density of aquaporins and varies with the cell type.

Osmotic pressure can be computed based on the concentration of various molecular species in the medium (see **Box 1**). To find the hydrostatic pressure difference one can mechanically model the cell as a semi-rigid envelope comprising the membrane and the cortex and containing a polymer meshwork (the cytoskeleton and other polymers) permeated by water (**Figure 1**). The balance between external and internal forces at the cell contour then takes the form

$$\sigma_{cyt} + \sigma_{cont} = -p^e + \sigma_{conf} \quad (2)$$

On the left-hand side,  $\sigma_{cyt} = \sigma_{mesh} - p^c$  is the mechanical stress in the cytoplasm, which is given by the difference between the stress in the cytoskeleton meshwork  $\sigma_{mesh}$  and the hydrostatic pressure in the cytosol,  $p^c$ , and  $\sigma_{cont}$  is a surface-tension term accounting for the resistance of the cell contour, comprising the membrane and cortex.

Both  $\sigma_{mesh}$  and  $\sigma_{cont}$  are related to cell deformations via the so-called constitutive behaviours (that is, active visco-poro-elasticity) of the meshwork and the cell contour<sup>11,15</sup>. Such constitutive behaviours are actively regulated by the cell. For example, the active stress in the cytoskeleton is regulated by small molecules such as Rho-GTPases, and the meshwork stiffness by the number of crosslinking proteins<sup>16</sup>.

On the right-hand side of Eq. (2),  $p^e$  is the external hydrostatic pressure applied to the cell and  $\sigma_{conf}$  describes the confining stress due to the mechanical environment of the cell including, for example, a cell's neighbours in a tissue and the extracellular matrix. The hydrostatic pressure difference  $\Delta p$  is a fundamental driving force of the water flux through the cell, as seen in Eq. (1). It therefore couples the volume of the cell to its mechanical properties through a force balance at the cell contour, as expressed in Eq. (2). In the following, we will consider different examples of volume adjustments following this prescription.

#### *Rapid mechanical volume adjustment for cells with a stiff wall*

Cells contain impermeable osmolites — for example amino acids and derivatives, polyols and sugars<sup>17</sup> — that cannot be exported or imported on a short timescale. Their intracellular concentrations are fixed by the cell function and metabolism and can differ from the extracellular levels such that one could assume that  $\Delta\Pi \neq 0$  in Eq. (1). Then, for cell volume to reach a steady state, such an imbalance should be absorbed by  $\Delta p$ , which builds up some mechanical stress in the cell through the force balance in Eq. (2).

Plant cells and, to a lesser extent, bacteria and yeast, possess a solid wall capable of withstanding a considerable amount of mechanical stress (given by  $\sigma_{cont}$  in Eq. (2)) with a small elastic deformation<sup>18</sup>. This enables them to offset the existence of a difference of osmolarity across their wall by mechanically balancing the imposed osmotic pressure difference with a hydrostatic pressure that equals the mechanical stress in the cell contour. Because the internal osmotic pressure can reach values as high as several atmospheres for plant cells, this mechanism requires considerable stiffness in the cell wall. For example, the Young's modulus of the cell wall of *Camellia* pollen tubes was estimated to be of the order of several hundred MPa<sup>19</sup>, similar to that of rubber.

### *Rapid osmotic volume adjustment of cells with channels and pumps*

For cells without a rigid wall, it has been argued<sup>11</sup> that the bulk cytoskeleton offers more mechanical resistance (given by  $\sigma_{mesh}$  in Eq. (2)) than the membrane and cortical layer, as it occupies a larger volume. However, the cytoskeleton would still have insufficient stiffness to accommodate the magnitude (up to one atmosphere) of an osmotic pressure difference across the cell membrane typically imposed during an osmotic shock, i.e. a sudden change of the external concentration of an osmolyte impermeable to the cell membrane (**Figure 2a, b**). Early experiments on red blood cells show that, under such shock, the cell volume reaches a new value in a fraction of a minute, apparently acting like an osmometer<sup>20</sup>.

The cell volume after the shock is related to the magnitude of the shock through Ponder's relation, which can be deduced from the pump-and-leak mechanism<sup>21,22</sup>. A simplified explanation of this mechanism involves a pair of small ions (typically sodium and potassium) travelling through selective channels and pumps. The differential permeability of the membrane with respect to each ion, working in tandem with pumps exchanging the ions at a fixed rate, offsets the difference of impermeable osmolyte concentrations to maintain  $\Delta\Pi = 0$  in Eq. (1), preventing cell lysis (explained in detail in **Box 2**). As a result, a change of ion permeability can affect the cell volume. For example, inhibition of p38 MAP kinase increases membrane  $\text{Na}^+$  permeability and consequently the cell volume of HTC liver cells<sup>23</sup>. Notably, some large macromolecules can have an important indirect contribution to the osmotic pressure if they carry a substantial amount of negative charges, which must be balanced by counter ions. Such electro-osmotic effects can be taken into account leading to a more quantitative albeit more complex picture.

These volume changes also require a cell surface adaptation. The cell membrane is a floppy structure in which excess surface is stored in wrinkles and in other structures such as caveolae<sup>24</sup>. When the volume change is too fast, the membrane detaches from the underlying cortex, and rupture occurs if the total volume exceeds the total available membrane surface area. This can be exploited experimentally to measure stored surface<sup>25</sup>. For slower volume changes, for example low permeability of the cell to water, the cell surface can adapt by addition or removal of lipids by endocytosis or exocytosis.

### *Regulatory volume adaptation*

Most mammalian cells, following their initial volume change in response to an osmotic shock, are able to regain their volume preceding the shock<sup>12</sup> over a typical timescale of 10 minutes (**Figure 2a, c**). The effect of a hydrostatic pressure compression can involve a substantial volumetric decrease over the same timescale<sup>26</sup>. Upon spreading on a substrate, cells also lose volume on a similar timescale<sup>5</sup> and during mitosis, cells significantly increase their volume as they round up<sup>27,28</sup>. These regulatory responses to biomechanical perturbations are accompanied by fluxes of osmolytes, typically small ions, through the cell membrane, revealing the existence of a coupling between the osmotic and mechanical balance, whose biological importance may be crucial for other aspects of cell physiology. For example, cells have a higher rate of viability upon an osmotic shock when they are mechanically constrained by their neighbours in a monolayer than when they are in suspension<sup>29</sup>. The mechanisms at play in such regulatory processes are still poorly understood<sup>12,30</sup>.

Volume regulation can involve mechanosensitive channels on the cell membrane, which open in response to increased tension<sup>31,32</sup> and couple the cell volume to the cell surface area (see **Box 3**). Owing to the fact that ion permeabilities (typically  $10^{-8}$  cm/s<sup>33</sup>) through the membrane are orders of magnitude smaller than that of water ( $10^{-3}$  cm/s), the influence of such channels on the rate of volume change is slower than the initial response, which is purely osmotic. Consistent with

the idea that rates are important, it was<sup>34</sup> recently reported that a slow and moderate modification of the external ionic concentration in tumour cells does not lead to any regulatory response.

Mechanosensitive channels are represented in a wide variety of organisms such as bacteria, yeasts or *C.elegans*. In mammalian cells, the TRP family and others<sup>35</sup> are well studied, and piezo channels, important for a cell's response to applied forces, have been recently shown to participate in volume regulation<sup>36</sup>. Because of the floppiness of the plasma membrane, it is likely that the tension in mechanosensitive channels is mostly controlled by the cytoskeleton swelling or shrinking. The importance of cytoskeleton linkage to the membrane<sup>37</sup> was demonstrated for volume-regulated anion channels (VRACs<sup>38</sup>). The lipid composition and the ensuing local variations of the membrane may also play a mechanosensitive role<sup>30</sup>.

It is however not clear that the tension inflicted on a channel during a moderate osmotic shock is sufficient to account for the tension required to open the channel, as measured by patch-clamp experiments<sup>30,39</sup>. Another mechanism of volume adaptation is the modulation of the ion-pumping rate by non-mechanical factors<sup>30</sup>. For example, Na<sup>+</sup>/K<sup>+</sup> ATPase pumps are controlled by cAMP-dependent protein kinases. The activity of these kinases is itself controlled by a number of molecules that can be concentrated or diluted following osmotic volume changes. This could in turn modulate the endocytotic depletion of pumps from the plasma membrane and also regulate their pumping activity. In addition, molecular crowding, following a loss of water upon an hyperosmotic shock, could lead to a decrease in the metabolic activity of the pumps. Finally, the concentrations of some specific ions in direct chemical interaction with the pumps could also impact volume adaptation<sup>40</sup>.

Other than ions, some organic molecules are known to play the role of osmoregulators<sup>30</sup>. For example, in plants, the taurine content is governed by the osmolarity of the environment through the regulation of the synthesis of its transporter TauT<sup>41</sup>. Last but not least, another factor of cell-volume regulation is the contribution of voltage-gated channels<sup>42</sup>. In response to an osmotic shock, the membrane potential changes as the Gibbs–Donnan equilibrium is perturbed, and this may be sufficient to gate voltage-sensitive channels and change the ionic cell permeability.

### Cell-size homeostasis on timescales of one generation

We now consider the long timescale of growth and division. On this timescale, the average size of a cell is defined by how much it grows between two division events.

#### *Cell size in cycling versus non-cycling cells*

Cell mass and volume double on average at each cell cycle, and controlling fluctuations in a cell population from an average cell size requires a tight coupling of growth and division (**Box 4 and Figure 3e-f**). Classically, animal cells that no longer divide but are still metabolically active have a dry mass that balances mass accumulation with mass reduction<sup>43</sup>. The commonly accepted view casts the rates of protein synthesis and degradation as the downstream result of growth pathways that translate extracellular cues (such as amino acids and growth factors) and intracellular cues (such as energy status, oxygen and amino acids) into regulatory signals for growth (such as protein or lipid synthesis, protein degradation and cell autophagy) (**Figure 3a**). We refer the reader to other reviews for a description of the three most important growth pathways for mammalian cells, namely mTOR<sup>44</sup>, Myc<sup>45</sup> and Hippo<sup>9</sup>.

In this section, when we refer to cell size, we do not distinguish results obtained from dry mass, buoyant mass or volume measurements. Instead we assume that, on the timescale of the cell cycle, they should behave in a similar manner. However, as we will discuss, this is partly an open question. For some organisms with a simple shape, such as yeast and bacteria, most studies use volume as the size observable, as it can be extracted from the 2D outline of cells by assuming a prolate geometry. On the other hand, the volume of mammalian cells is more difficult to measure from the image of the cell outline, so most studies take either dry mass, protein content or buoyant mass (depending on the measurement method) as a size observable. Only two recent studies report direct measurements of volume of mammalian cells in the context of cell-size homeostasis over cycles of growth and division<sup>46,47</sup>.

#### *The typical and average growth law of single cells*

In proliferating populations of single-celled organisms, the number of cells grows exponentially in time. However, this clearly does not mean that the growth of the cells themselves follows the same law. Cells growing linearly in time and performing binary divisions still give rise to exponentially growing populations. Single-cell growth is exponential if the amount of material produced by the cell per unit of time is proportional to the number of intracellular molecular machines producing this material, and cell size is a proxy for this number.

Whether single-cell growth is better described by linear, exponential or some other faster- or slower-than-linear law remains a controversial question, even when data are abundant, as in bacteria and yeast (see below). This is due to the fact that the relative difference between exponential and linear single-cell growth is at most 6%, but also because it is challenging to measure cell size with such precision. Single-cell-growth curves may thus not give a clear answer. It is simpler to ask if the average growth speed computed over many cells of a given size increases with cell size<sup>48</sup> (**Figure 3b-d**).

Although these averages generally point to exponential growth, they may emerge from more complex behaviours at the single-cell level or in cell-cycle sub-periods. Most studies using classical image analysis to measure bacterial cell size conclude that exponential growth is a good description<sup>49,50</sup>, but a study performing high-resolution measurements of *E. coli* cells has proposed that their growth is bi-phasic<sup>51</sup>, a result also reported recently in *Bacillus subtilis*<sup>52</sup>. In budding yeast, the average growth rate was reported to change at regulatory checkpoints with the cell-cycle phase<sup>53,54</sup>. In *S.pombe*, a systematic study of single-cell growth concluded that although the majority of growth trajectories were best described by a bi-linear curve (**Figure 3b**), a small portion of the cells were better described by a linear or exponential curve<sup>55</sup>. In animals, most studies suggest that, on average, cells grow exponentially<sup>56-58</sup>. Others have found that, growth is linear<sup>59</sup> on average, but the variety of measurement methods and model systems used precludes a general conclusion.

#### *Linking the mathematical growth law to the biology of growth*

The growth mode reveals important aspects of the biological processes that drive cell growth. In *S.pombe*, the bi-linear growth model was related to the 'new end take off' after which growth occurs at both poles instead of the old pole only<sup>60</sup>. Later studies suggested that it instead correlated with completion of DNA replication<sup>61</sup>. It is also possible that the phase-dependent changes in growth rates observed in budding yeast<sup>54</sup> or in mammalian cells<sup>58</sup> are the consequence of preferential allocation of energy resources to either the replication and division machinery in S and M phase or the protein synthesis machinery during the two growth phases G1 and G2<sup>62</sup>. Alternatively, exponential growth could be driven by the production of new proteins from a pool of ribosomes, which itself increases proportionally to cell size<sup>63</sup>. However, upper bounds to this exponential growth mode could exist<sup>64</sup>,

for example because mitochondrial function in mammalian cells scales non-linearly with size<sup>65</sup> or due to the finite number of DNA copies<sup>66,67</sup>. A better understanding of what drives (and limits) cell growth is a challenge for future studies of cell-size regulation.

#### *Coupling division rate to cell size*

Because most studies have reported faster-than-linear growth, simple cell-division dynamics relying solely on a cycle clock could not ensure a robust size distribution in a population (see **Box 4**). Consequently, the question of size control over generations has taken centre stage. In unicellular organisms, cell-cycle duration is negatively correlated with cell size at birth<sup>49,68</sup>, meaning that size homeostasis could rely on a modulation of cell-cycle progression (as reviewed in ref. <sup>69,70</sup>). In animal cells, similar to budding yeast<sup>68,71</sup>, a series of indirect approaches performed at the population level<sup>72,73</sup> and direct measurement on single cells<sup>47,74</sup> have reported evidence of changes in the length of the G1 phase of the cell cycle as a function of cell size at birth. One study recently suggested that p38 is the central player in controlling size-dependent duration of G1 in HeLa cells<sup>73</sup>. It should be noted, however, that the negative correlation between G1 and cell size at birth was relatively weak. Although initial works focused on one specific cell-cycle checkpoint, at which division rate and cell size were coupled, recent findings in various organisms, such as *S.cerevisiae*<sup>75,76</sup> and animal cells<sup>47</sup>, instead suggest that coupling is achieved at several different times in the cell cycle. The relative importance of these independent checkpoints is thought to depend, at least partly, on environmental factors determining growth rate<sup>77</sup>.

#### *Molecular mechanisms coupling division rate with cell size*

From bacteria to animal cells, the question of the molecular factors affecting size sensing is currently a subject of active research<sup>69,70</sup>. We briefly discuss two basic theoretical prototypical models that are often invoked in the recent literature.

The 'inhibitor dilution' model<sup>78</sup> hypothesizes that an inhibitor of cell-cycle progression, which is not produced proportionally to a cell's size, gets diluted to a critical value by volume increase. Division occurs at a target size, a type of size control called a sizer. A variant of this model for asymmetrically dividing cells<sup>79</sup> produces a nearly constant added size between divisions, which is called an adder. The most delicate hypothesis in this class of model is what sets the initial number of molecules of the inhibitor. Dilution of the inhibitor Whi5 has been implicated in the budding-yeast G1-S transition<sup>80</sup>, whereas recent evidence suggests that the same mechanism might be at play in cultured mammalian cells with Rb in a central role<sup>81</sup>.

The 'initiator accumulation' model<sup>82</sup> assumes that an initiator molecule reaches a critical amount or concentration. The initiator might be produced at a rate proportional to cell volume and the threshold is a critical number of initiator molecules, which gates the transition through the next cell-cycle phase. If the initiator is halved at (symmetric) cell division, as it would be natural for a protein, then the initiator triggers division at a fixed size threshold (and thus is a sizer). In *E. coli*, the septum could act as an 'initiator' bottleneck for cell division. In this case surface material is likely produced at a rate proportional to volume, and a new septum must be produced from zero for the cell to divide, leading to near-adder behaviour<sup>83</sup>. Another finding potentially in line with the initiator accumulation category of model is the growth-rate dependent accumulation of E2F factor in endocycling cells from *Drosophila* salivary gland, which triggers transition through S phase in a dose-dependent manner<sup>84</sup>. It is important to note that, because most molecular processes work through concentrations and not absolute numbers, the hypothesis of a critical number gating cell-cycle transitions is not trivial<sup>82</sup>. In fission yeast, an accumulator circuit seems to use protein localization dynamics to sense area<sup>75</sup> whereas in *S. cerevisiae* an alternative to the size-sensing mechanism based on Whi5 dilution has

been suggested to rely on the titration of the mitosis activator Cln3 against a fixed number of genomic binding sites<sup>85</sup>.

#### *Growth-rate modulations throughout the cell cycle*

In addition to — or instead of — a coupling between the cell-cycle time and cell size or growth, a modulation of growth speed or rate could also achieve size homeostasis at the cell population level. In this case, even with a constant cell-cycle duration, coupling between growth dynamics and size would allow smaller cells to grow more than (or at least as much as) their larger counterparts, despite exponential growth. Available data seem to rule out this kind of control for microorganisms<sup>86</sup>. However, for mammalian cells, the hypothesis was put forward based on indirect evidence<sup>56</sup>.

One major limitation is the difficulty in producing reliable single-cell growth curves over complete cell cycles. Studies based on measures of single cells at a single time point require strong assumptions to reconstruct growth trajectories<sup>56,57,87</sup>. Sophisticated techniques now allow single-cell measures over complete cell cycles<sup>46,47,58,88</sup>, but the number of observations is still limited. Together these studies suggest (in different forms) a contribution of growth-speed modulation to cell-size homeostasis. Some studies have found growth speed to be cell-cycle phase dependent<sup>58</sup>, or to show a reduced variability at the G1/S transition<sup>46</sup>. Size homeostasis could also be achieved if large cells grow slower than small ones at this transition<sup>56,89</sup>. Alternatively, even if the average growth speed increases linearly with cell size (thus being on average exponential), the rate of increase might vary with volume at birth<sup>47</sup>. In addition to the challenge of producing good measurement datasets for growth fluctuations at the single-cell level, there is a need for the development of theoretical tools that quantify the contribution of these fluctuations to the effective homeostasis mechanism.

#### *Mathematical formalisms to describe the coupling of division- and growth-rate modulations*

Discrete-time equations based on the unit of the cell cycle and an auto-regressive process of sizes across generations can describe the coupling of division rate to cell size<sup>50,79,90</sup> (see **Box 4**). This formalism can be used to evaluate the respective contributions of the modulation of growth and cycle timing on effective size control<sup>47</sup>. Comparing experiments on single mammalian cells with a global analysis of yeast and bacteria datasets shows that modulations of growth rate might be more specific to animal cells<sup>47</sup>. Alternatively, one can study the hazard division rate function  $h_d$ , defined as the rate of division of undivided cells as a function of time and other key variables, for example the size of the cell, initial size and nuclear size (see discussion below). This quantity has the advantage of not requiring any *a priori* hypothesis on the nature of the coupling between division rate and cell size<sup>49,50,91,92</sup>. Instead, the division rate is inferred directly from data, by conditional histograms estimating the probability of dividing at fixed values of time, size or any other measured variable. This approach can capture relevant details<sup>91</sup>, but it is difficult to relate to simple underlying mechanisms and requires large datasets. This formalism might prove interesting for future studies focusing on detailed aspects of cell-cycle progression, provided that effective methods for inference of  $h_d$  are developed.

Currently, two methodologies can assess  $h_d$ . Naïve inference of the hazard rate from conditional probabilities requires a large amount of data and more advanced inference methods are possible<sup>93</sup>, but they have not been widely used in the field so far. Thus, the alternative approach<sup>67,94</sup> of considering all the possible correlations measured in single cells between size parameters and cell-cycle timing and relating them to discrete-time processes has been more successful. This method has been particularly effective when measurements of cell-cycle intervals were available, for example in investigations on the relation between replication initiation and the cell cycle<sup>47,74,79,80</sup>. In such

studies, the joint use of single-cell data and mathematical models has led to the proposal of specific mechanisms of cell-cycle progression.

However, we still lack a unified method to account for all the measured correlations, which has led to conflicts in the interpretation of the data<sup>95</sup>. Indeed, single-cell dynamic data offer many correlation patterns that are often difficult to interpret. In *E. coli*, which represents most of the currently available datasets, the latest analyses challenge the classic tenet that completion of chromosome segregation is the rate-limiting process for cell division. Rather, two concurrent processes — an inter-division process (septum completion) and a replication-related process — compete to determine cell division. If confirmed, these results would support a novel view of how different processes are coordinated by the cell cycle, in which the key aspect of cell-cycle transitions is the downstream integration of the result of concurrent processes rather than the upstream scheduling by a ‘master clock’.

### **The future of cell-size research**

A number of questions remain to be answered in ongoing efforts to understand cell-size regulation.

#### *Coupling growth of size parameter with physical feedback mechanisms*

The ideas presented in the previous two sections might seem distant from each other: fast water exchange and force balance on the cell boundary versus slow growth and division events. However, they are intimately connected, because the short-timescale biophysical processes are constantly at work to set the instantaneous cell-size parameters for the contents of a given cell. These may include its volume and thus concentrations, or its surface area. Fast dynamics of cell mass have also been recently reported<sup>96</sup>. This instantaneous cell state, which is the result of past growth, is thus likely to feedback on the future growth parameters of the cell. But how the coupling between long and short timescales operates is currently not understood.

#### *Joint control of cell growth by biological and mechanical factors*

During the cell cycle, responding through specific pathways to the availability of nutrients and growth factors that control active processes, cells increase their dry mass by accumulating proteins<sup>28</sup>. On average, the DNA and protein content have been shown to be proportional to the cell volume<sup>97,98</sup>. Physically, this may be due to the import of amino acids and other metabolites, which slowly increases the internal number of impermeable macromolecules and hence the volume (see Eq. (2-1) in **Box 2**). Other physical parameters such as the ions pumping rate, membrane potential<sup>99</sup> and mechanical tension in the cytoskeleton controlling the cell permeability could be regulated fast enough to remain quasistatic at the timescale of the cell cycle. In support of such timescale separation, the long-term volume growth of *Escherichia coli* was shown to be independent of small osmotic perturbations<sup>100</sup>. However, volume recovery after osmotic shocks of large magnitude requires the protein synthesis of channels and pumps<sup>101</sup>, and this suggests that there exists a coupling between short- and long-timescale volume homeostasis, at least under extreme conditions. Indeed, transcription of more than 500 genes is induced within the initial 10 minutes of an osmotic shock<sup>102</sup> and in yeast, osmotic stress is well known to affect the MAPK Hog1 kinase, which controls transcription factors<sup>103</sup>.

Cell-volume changes also affect genetic expression<sup>104</sup> and protein synthesis<sup>105</sup>, as well as protein–protein interactions<sup>106</sup>. One hypothesis is that molecular crowding is actively tuned to a critical value insuring an optimal tradeoff between the local availability of catalytic units such as ribosomes<sup>107</sup> and

the possibility of diffusive transport inside the cytoplasm, crucial for various biochemical reactions<sup>108</sup>. In support of this idea, density has been reported to fluctuate much less than volume<sup>109</sup>. Moreover, forcing cells to operate far from this optimal density dramatically impairs essential cell functions<sup>1</sup>.

On a long timescale, the surface growth rate may also be a limiting factor of cell volumetric and mass growth. Although direct evidence is still lacking for mammalian cells, for plant cells and bacteria, volumetric growth is limited by the surface growth of the wall such that the cell shape is strongly linked to the cell volume<sup>83</sup>. For example, a slow increase of the turgor pressure in tobacco pollen tubes increases the tension in the wall and promotes addition of pectin components and thus cell elongation. However, the direct role of the turgor pressure is debated, because the underlying molecular mechanisms resulting in the wall growth have not been fully clarified<sup>110</sup>. In mammalian cells, as in yeast and bacteria, multiple mechanisms act at all timescales to produce feedback between surface-tension parameters and surface extension<sup>111,112</sup>. These phenomena of surface homeostasis, coupling mechanics and growth, are still largely unexplored and could be central regulators of cell growth.

#### *A deeper view of single-cell growth*

Considering biophysical feedback on cell growth makes the question of single-cell growth more complex and intriguing than assumed by considering only the biological factors of synthesis and the degradation of components. Increasing the accuracy and throughput in producing single-cell growth curves will be crucial in this respect. The parallelization of a technique involving suspended microchannel resonators now allows high-throughput measurement of buoyant cell mass<sup>113</sup>, together with single-cell RNA sequencing<sup>114</sup>. Other approaches aiming at simplifying the experimental set-up are also promising<sup>115,116</sup>. In animal cells, evidence suggests that growth rate could be modulated not only through external signals, such as growth factors and nutrients, but also as a function of cell size itself<sup>47,89</sup>. However, the chemo-mechanical processes and size parameters involved in this coupling remain unknown.

We can sketch a hypothetical working model that couples the various size variables and timescales (**Figure 4a**). Dry mass depends on synthesis rate, which may be modulated by a set of factors including external signals (nutrients, mechanical forces). Cell-surface-area expansion is limited by synthesis of plasma-membrane components on the timescale of hours, whereas endocytosis and exocytosis limit surface expansion at intermediate timescales (minutes) and membrane reservoirs and folds and their interaction with the dynamic cell cortex dominate at short timescales (seconds). Volume is coupled to surface area via cell shape (and thus spreading area), owing to mechanisms of surface-tension homeostasis regulating the cell permeability and ion pumping, which control the osmotic response. This coupling of volume to surface then modulates density and macromolecular crowding at short timescales, which itself feeds back on synthesis, through density homeostasis mechanisms or direct modulation of signalling dynamics. In a population of proliferating cells, a coupling of these size parameters with the cell-division-cycle clock maintains the distribution of cell sizes constant through generations.

#### *Coordination of tension and growth in gram-positive bacteria*

The example of gram-positive bacteria<sup>110</sup>, makes the above scheme more precise. This study identifies key factors in the balanced synthesis of subcellular components during cell growth by looking at the response behaviour to osmotic shocks (**Figure 4b**).

In these bacteria, cell volumetric growth is driven by the peptidoglycan wall, a thick structure which supports the plasma membrane, itself controlling cell permeability. Following a hypoosmotic shock, water swells the bacteria, increasing the internal turgor pressure, which elastically stretches the wall on a short timescale and subsequently increases the membrane tension. This increase in tension decreases its permeability with respect to wall precursors and slows down the growth on an intermediate timescale. As growth slows down, tension in the membrane decreases as membrane synthesis increases, re-establishing a target membrane tension that itself drives cell-wall precursors back to their homeostatic concentration to recover, on a long timescale, the initial growth rate. In this situation, the external perturbation is buffered across various timescales to re-establish the initial growth rate.

The importance of short-timescale regulatory processes is highlighted by the fact that a hyperosmotic shock has a long-timescale signature on growth. In this case, the cell is quickly compressed by the external pressure leading to a decrease in the membrane tension and a subsequent increase in its permeability. The flux of cell-wall precursors is stopped in the periplasm and cell-wall synthesis is inhibited, resulting in a permanently impaired growth rate on a long timescale. Growth is henceforth seen as the result of equilibrium between biophysical 'restoring forces' and biochemical or biological factors.

#### *Conclusive remarks*

Cell volume can be understood as an almost instantaneous osmotic balance between impermeable and permeable osmolites, modulated by slower regulatory increase or decrease aiming to re-establish several cellular quantities (such as surface tension). Fast external perturbations are thus buffered by regulatory processes while the dry mass content of the cell slowly increases at the timescale of the cell cycle. In this picture, volume follows mass, responding to the slow increase of internal impermeable molecules to maintain a homeostatic mass density of the cell necessary for its proper physiological function. In turn, dry mass, concentration and crowding in both the nucleus and the cytoplasm may affect biosynthesis processes. The growth rate would then result from the integration of all the above processes and a possibly large set of as-yet uncharacterized feedbacks over the cell cycle, with some details becoming irrelevant in the averaging of small timescales into large timescales. Meanwhile, a set of processes related to size parameters might feed into the decision of the cell to divide, also affecting size homeostasis over subsequent generations. Identifying the minimal set of variables and their underlying dynamics to obtain a state equation, ruling the size of cells during the cell cycle remains an open problem.

## Figure Legends:

### Figure 1: Factors setting the steady-state cell volume

For a mammalian cell (left) or a walled cell (right), water is driven through selective water channels (aquaporins) according to the hydrostatic and osmotic pressures (see **BOX 1**). Osmotic balance is controlled by ion channels and ATP driven pumps (bottom right box). Hydrostatic pressure is set by the force balance on the cell envelope. Cytoskeleton meshwork mechanical stress  $\sigma_{mesh}$  combines with the internal hydrostatic pressure  $p^c$  to build the effective stress  $\sigma_{cyt}$  in the cytoplasm (middle left box). Surface tension  $\sigma_{cont}$  is generated by the membrane and the actomyosin cortex or wall (top right and bottom left boxes). Tension regulation endocytosis and exocytosis modulate surface area (top left box). Internal mechanical stress balances the external confining stress  $\sigma_{conf}$  and hydrostatic pressure  $p^e$  applied to the cell contour.

### Figure 2: Cell-volume regulation at short and medium timescales

- a. Cell volume during hypotonic shock of HBE cells (adapted from ref. <sup>117</sup>).
- b. Fast passive swelling after hypotonic shock occurs when low extracellular osmolality generates water influx through aquaporins (top box). This detaches the actomyosin from the plasma membrane, unfolds the membrane and increases  $\sigma_{cont}$  (bottom box).
- c. Regulatory volume decrease (RVD) occurs when ion pumps, activated by the swelling change the osmotic balance (top left), induce expulsion of water from the cell (top right). The actomyosin cortex reassembles on the plasma membrane and refolds it (bottom left), while a balance between endocytosis and exocytosis adjusts the surface area (bottom right).

### Figure 3: Cell-volume regulation at medium and long timescales

- a. Three basic processes involved in cell growth include (from left to right) net import of extracellular material and a balance between synthesis and degradation, extension of the plasma membrane by a balance between endocytosis and exocytosis, and water entry and the activity of ion channels.
- b. Single-cell growth curves across a full cell-division cycle. Left: *S.pombe* length growth curve (data from ref. <sup>118</sup>). Red lines: bi-linear fit. Dashed line: new end take-off. Right: HeLa cell volume growth curve (data from <sup>47</sup>) obtained with FXm measurement. Dashed circle point to short time fluctuations (the second at top right corresponds to mitosis, see <sup>27</sup>). Crosses: raw measurements, red lines: sliding average.
- c. Average growth behaviour. Left: Examples of individual growth curves obtained in *E. coli* (data from ref. <sup>92</sup>). Grey lines are curves for individual cells, red line is the average of all the curves. Right: Plot of size as a function of time representing schematic linear growth curve (dashed line) and exponential growth curve (solid line). Growth speed is the derivative of this plot on single cells.
- d. Coupling of growth with cell-cycle progression. Left: Growth speed extracted from single curves as shown in c. Squares represent the conditional average of growth speed on size, the dark line is a linear regression on the average bins. Right: Schematic plot of growth speed as a function of size, the slope of this relationship yields the average growth rate. In the case of linear growth (dashed line), this rate vanishes, whereas in the case of mono-exponential growth, it is positive and constant.

**e-f.** In order to maintain size homeostasis in proliferative cells, growth and cell-cycle progression must be coupled. This can be achieved either by **e)** modulating the division rate or **f)** modulating growth rate, as a function of cell size.

**Figure 4: Illustration of the timescales at play in the regulation of cell-size parameters**

**a. Left top**, from ref. <sup>119</sup>: Transfer of neutrophil to water induces passive fast water movement across the membrane, resulting in progressive swelling and following by cell lysis.

**Left bottom**, from ref. <sup>96</sup>: At short timescales (second to minutes), physical and mechanical properties are central and cell mass can be considered almost constant, although significant fluctuations have been observed compared with fixed cells.

**Middle top**, from ref. <sup>61</sup>: Elongation of individual *S.pombe* cells from birth to subsequent division.

**Middle bottom**, from ref. <sup>120</sup>: Nutrient depletion by exchanging the media to PBS-suppressed mass accumulation rate, whereas exchanging the cell back into normal nutrient-containing media restores mass production.

**Right top**, from ref. <sup>27</sup>: Cell volume before mitosis is almost twice that at birth. During mitosis cells additionally increase their volume by 30%.

**Right bottom**, from ref. <sup>58</sup>: G1-, S-, and G2-dependent dry-mass growth during the cell cycle. Cell-cycle phases are indicated by colour.

**b.** Schematic of the tension–inhibition model presented in ref. <sup>112</sup>, explaining hypoosmotic-shock-induced growth inhibition. The model is consistent with experimental data obtained for different magnitudes of osmotic shock.

### BOX 1: Fluxes at the cell membrane

A cell (volume  $V_c$ ) contains a solvent (mass density  $\rho$ ) under hydrostatic pressure  $p^c$  and solute species that are either permeable (mass fraction  $\phi_p^c$ ) or impermeable (mass fraction  $\phi_i^c$ ) to the cell membrane (see also<sup>13</sup>). Similarly, the extracellular medium (volume  $V_e$ ) is under pressure ( $p^e$ ) and its species mass fractions ( $\phi_p^e, \phi_i^e$ ) can be controlled externally. A particular feature of the cell is that it contains ATP, which is perpetually hydrolyzed (to some extent  $\zeta$ ) to 'feed' the ion pumps. The mass fraction of each of these species satisfies simple conservation laws:

$$\frac{dV_c}{dt} = J_w, \rho \frac{d(\phi_p^c V_c)}{dt} = J_p, \rho \frac{d(\phi_i^c V_c)}{dt} = 0 \text{ and } \rho V_c \frac{d\zeta}{dt} = S_\zeta,$$

where  $J_w$  and  $J_p$  are the fluxes of solvent and permeable species inside the cell and  $S_\zeta$  the rate of the ATP hydrolysis. Total conservation of water and molecular species ensures that  $V_c + V_e$ ,  $\phi_p^c V_c + \phi_p^e V_e$  and  $\phi_i^c V_c + \phi_i^e V_e$  are constants. The fluxes expressions can be complex but they have to satisfy a fundamental thermodynamic inequality<sup>121</sup> which for an isothermal system reads:

$$\mathcal{D} = \frac{dW}{dt} - \frac{dF}{dt} \geq 0,$$

where  $\mathcal{D}$  is the dissipation,  $dW/dt = -p^e dV_e/dt - p^c dV_c/dt$  is the rate of mechanical work performed on the system and  $F = \rho V_c f_c(\phi_p^c, \phi_i^c, \zeta) + \rho V_e f_e(\phi_p^e, \phi_i^e)$  its total free energy with  $f_c$  and  $f_e$  the free energies per unit mass respectively within and outside the cell. Using the conservation laws, we obtain  $\mathcal{D} = J_w(\Delta p - \Delta \Pi) + J_p \Delta \mu_p + A S_\zeta$ , where  $\Delta h = h^e - h^c$  denotes the difference of the considered quantity  $h$  between the cell and the extracellular medium,  $\mu_{p,i}^{e,c} = \partial f_{e,c} / \partial \phi_{p,i}^{e,c}$  are chemical potentials,  $\Pi^{e,c} = \rho(\phi_p^{e,c} \mu_p^{e,c} + \phi_i^{e,c} \mu_i^{e,c} - f_{e,c})$  osmotic pressures and  $A = -\partial f_c / \partial \zeta$  the affinity of the ATP hydrolysis which is assumed constant as in the active gel theory<sup>122</sup>.

Close to thermodynamic equilibrium, following the Onsager principle, generalized fluxes can be related to generalized forces through a symmetric positive matrix  $\Lambda$  of kinetic coefficients<sup>121</sup>, such that  $\mathcal{D}$  remains positive

$$\begin{pmatrix} J_w \\ J_p \\ S_\zeta \end{pmatrix} = \begin{bmatrix} \Lambda_{11} & \Lambda_{12} & \Lambda_{13} \\ \Lambda_{12} & \Lambda_{22} & \Lambda_{23} \\ \Lambda_{13} & \Lambda_{23} & \Lambda_{33} \end{bmatrix} \begin{pmatrix} \Delta p - \Delta \Pi \\ \Delta \mu_p \\ A \end{pmatrix}$$

The classical assumptions are that aquaporin channels are selective ( $\Lambda_{12} = 0$ ) and passive ( $\Lambda_{13} = 0$ ) and the water flux inside the cell reads  $J_w = \Lambda_{11}(\Delta p - \Delta \Pi)$  where  $\Lambda_{11} = L_p$  is the filtration coefficient of the cell membrane. The flux of permeable species inside the cell reads  $J_p = \Lambda_{22} \Delta \mu_p + \Lambda_{23} A$ , where the first term is the classical Fick law and the second term (sign indefinite) describes the work of the pumps.

If the cell internal and external media are sufficiently dilute, the expressions of the osmotic pressures and chemical potentials can be derived from the nonlinear dependence of the free energy,  $f(\phi) = RT(\phi \log \phi - \phi)/M$ , where  $R$  is the gas constant,  $M$  is the molecular mass of the solvent and  $T$  is the temperature, leading to Van't Hoff law,  $\Delta \Pi = \rho RT(\Delta \phi_i + \Delta \phi_p)/M$  and  $\Delta \mu_p = RT \log(\phi_p^e / \phi_p^c)/M \simeq RT \Delta \phi_p / M$  when  $\phi_p^e$  and  $\phi_p^c$  are close enough. Molecular crowding and volume exclusion inside the cell are challenging to take into account, but are often represented by a simple prefactor.

### BOX 2: Prototypical example of a pump-and-leak model

Neglecting the hydrostatic contribution in Eq. (1) (main text), the flux of water is driven by the osmotic pressure which can be divided into an impermeable and a permeable contributions,  $\Delta\Pi = \Delta\Pi_p + \Delta\Pi_i$  (see **BOX 1**)<sup>21,22</sup>. For simplicity, we consider only a couple of permeable molecules (ions), denoted  $-$  (for the actively exported) and  $+$  (for the actively imported) and neglect electrostatic effects. Then, the incoming fluxes of ions can be approximated by (see **BOX 1**)

$$J_+ = \alpha_+ \Delta\Pi_+ + J_a \text{ and } J_- = \alpha_- \Delta\Pi_- - J_a$$

where the ionic channels' passive permeabilities are  $\alpha_+ \geq \alpha_-$  and we assume the same rate of active import and export  $J_a \geq 0$ . In steady state, the net flux of both ions remains zero, thus the variations of osmotic pressures of permeable and impermeable species read

$$\Delta\Pi_p = \Delta\Pi_- + \Delta\Pi_+ = J_a \frac{\alpha_- - \alpha_+}{\alpha_- \alpha_+} \text{ and } \Delta\Pi_i = k_B T \left( \frac{N_i^c}{V_c} - C_i^e \right)$$

where  $k_B$  is the Boltzmann constant,  $N_i^c$  is the number of impermeable osmolites in the cell and  $C_i^e$  is the controlled external concentration of impermeable osmolites. The steady-state ( $J_w = 0$ ) cell volume

$$V_c = \frac{N_i^c}{C_i^e + \frac{J_a}{k_B T} \frac{\alpha_+ - \alpha_-}{\alpha_- \alpha_+}} \quad (2-1)$$

is proportional to the amount of impermeable osmolites present in the cell and inversely proportional to the external concentration and the pumping rate. It is also possible to add a small osmotically insensitive volume  $V_0$  at the right-handside of the above formula to account for steric interactions under high osmotic compression. Eq. (2-1) is reminiscent of a Van der Waals equation of state and has been experimentally verified<sup>10</sup>.

### BOX 3: Prototypical example of mechanosensitive volume homeostasis

From the prototypical pump-and-leak model (see **BOX 2**) and assuming for simplicity that the ionic permeability of the membrane has a mechanically insensitive part  $\alpha$  and, for the imported ionic species only, a mechanically sensitive part  $\delta\alpha \ll \alpha$ , Eq. (2-1) relates the external osmotic pressure of impermeable molecules  $\Pi_i^e$  to the cell volume:

$$\Pi_i^e = \frac{k_B T N_i^c}{V_c} - J_a \frac{\delta\alpha}{\alpha^2}. \quad (3-1)$$

Although the mechanical stress does not directly enter Eq. (3-1) since  $\Delta p$  has been neglected in Eq. (1) (main text), it can indirectly play a crucial role because the permeability  $\delta\alpha(\sigma_{cont})$  depends on the stress in the cell cortex and membrane<sup>31</sup>. It takes a large value  $\delta\alpha_L$  if  $\sigma_{cont}$  exceeds a critical value  $\sigma_{crit}$  corresponding to the opening of the ionic channels and a small value  $\delta\alpha_s < \delta\alpha_L$  if the channels are closed when  $\sigma_{cont} < \sigma_{crit}$ . Using Eq. (2) (main text), the stress in the cell contour can be related to  $\sigma_{mesh}$ , which can in turn be expressed as a function of the cell volume through the active visco-poro-elastic constitutive behaviour of the cytoskeleton. Such a relation, which we do not specify here, translates the critical condition for opening and closing channels to a critical condition on the value of the cell volume,  $V_{crit}$ , leading to

$$V_c = \begin{cases} \frac{k_B T N_i^c}{\Pi_i^e + \frac{\delta \alpha_s J a}{\alpha^2}} & \text{if } V_c < V_{crit} \\ V_{crit} & \text{if } V_c = V_{crit} \\ \frac{k_B T N_i^c}{\Pi_i^e + \frac{\delta \alpha_l J a}{\alpha^2}} & \text{if } V_c > V_{crit} \end{cases} \quad (3-2)$$

This equation features two expressions corresponding to the different ionic permeabilities when the mechanosensitive channels are closed and open, connected by a homeostatic volume  $V_c = V_{crit}$ , which is independent of the external osmolarity. It is straightforward to generalize this model to the non-zero  $\Delta p$  case to couple the value of the homeostatic volume to a homeostatic mechanical tension in the cell contour using the Laplace law. Although there is some indication that such mechanical gating might be involved<sup>31</sup>, direct experimental evidence is still lacking.

#### BOX 4 - Coupling of cell cycle progression with cell growth.

If volume is decoupled from cell cycle duration, a simple timing mechanism does not guarantee a stable cell size of exponentially growing cells<sup>69,70</sup>. One reaches this conclusion looking at the fixed point of the equation relating initial volume  $V_0$  in subsequent generations, labelled by  $i$  and  $i+1$

$$2V_0(i+1) = V_f(i) = V_0(i) e^{\alpha\tau}, \quad (4-1)$$

where  $\alpha$  is the growth rate and  $\tau$  is the inter-division time. For a timer,  $\tau = \tau^* + \xi$ , where  $\xi$  is stochastic noise representing cell-to-cell variability, and Eq. (4-1) can be rewritten for logarithmic size as

$$q(i+1) = q(i) + (\alpha\tau^* - \log 2) + \alpha\xi \quad (4-2)$$

where,  $q(i) = \log V_0(i)$  and we assume for simplicity that the growth rate  $\alpha$  is constant. Eq. (4-2) shows that  $\alpha\tau^* = \log 2$  in order to have a fixed point, but the size still performs a random walk, which does not attain a steady distribution.

In the general case where  $\tau$  may be coupled to size, Eq (4-1) can be written as

$$q(i+1) = q(i) + g(q(i) - \langle q \rangle) + \xi \quad (4-3)$$

For small size fluctuations, one can use the Taylor expansion of the function  $g$  around zero, and call the linear coefficient  $-\lambda$ . This parameter can be measured as the slope of the size-growth plot relating initial size ( $\log V_0$ ) and net growth ( $\alpha\tau = \log(V_f/V_0)$ ) of a cell. When  $\lambda = 0$  there is no size control (timer), when  $\lambda > 0$  there is some size control. The linearized equation reads

$$\delta q(i+1) - \delta q(i) = -\lambda \delta q(i) + \xi \quad (4-4)$$

where  $\delta q = q - \langle q \rangle$ . Eq. (4-4) shows that only for  $\lambda > 0$  (that is, in all cases except a simple timer), the fluctuations can converge to zero. Analogous reasoning for linear growth leads to the existence of a fixed point in case of a timer. More generally, the existence of a fixed point for initial volume is a necessary condition, and one also has to verify the role played by noise, that is, the stochasticity of single-cell behaviour. A fairly general discussion of convergence conditions for binary divisions and exponentially growing cells is given in ref.<sup>91</sup>, assuming additive noise as in Eq. (4-3). However, things could be more complex for non-binary divisions<sup>79</sup> for fluctuating or size-coupled growth rates, and for growth that is more general than exponential or linear<sup>47</sup>.

## Acknowledgements

MP was funded by Institut Curie and CNRS. LV has received funding from the European Union's Horizon 2020 research and innovation programme under the Marie Skłodowska-Curie grant agreement No 641639. PR acknowledges support from a CNRS Momentum grant.

## Bibliography

1. Miermont, A. *et al.* Severe osmotic compression triggers a slowdown of intracellular signaling, which can be explained by molecular crowding. *Proc. Natl. Acad. Sci.* **110**, 5725–5730 (2013).
2. Delarue, M. *et al.* mTORC1 Controls Phase Separation and the Biophysical Properties of the Cytoplasm by Tuning Crowding. *Cell* **174**, 338–349.e20 (2018).
3. Lecuit, T. & Lenne, P.-F. Cell surface mechanics and the control of cell shape, tissue patterns and morphogenesis. *Nat. Rev. Mol. Cell Biol.* (2007). doi:10.1038/nrm2222
4. Fischer-Friedrich, E., Hyman, A. A., Jülicher, F., Müller, D. J. & Helenius, J. Quantification of surface tension and internal pressure generated by single mitotic cells. *Sci. Rep.* **4**, (2014).
5. Guo, M. *et al.* Cell volume change through water efflux impacts cell stiffness and stem cell fate. *Proc. Natl. Acad. Sci. U. S. A.* **114**, E8618–E8627 (2017).
6. Marshall, W. F. Cell Geometry: How Cells Count and Measure Size. *Annu. Rev. Biophys.* **45**, 49–64 (2015).
7. Brownlee, C. & Heald, R. Importin  $\alpha$  Partitioning to the Plasma Membrane Regulates Intracellular Scaling. *Cell* **176**, 805–815.e8 (2019).
8. Edgar, B. A. How flies get their size: genetics meets physiology. *Nat. Rev. Genet.* **7**, 907–916 (2006).
9. Yu, F.-X., Zhao, B. & Guan, K.-L. Hippo Pathway in Organ Size Control, Tissue Homeostasis, and Cancer. *Cell* **163**, 811–828 (2015).
10. Zhou, E. H. *et al.* Universal behavior of the osmotically compressed cell and its analogy to the colloidal glass transition. *Proc. Natl. Acad. Sci.* **106**, 10632–10637 (2009).
11. Sachs, F. & Sivaselvan, M. V. Cell volume control in three dimensions: Water movement without solute movement. *J. Gen. Physiol.* **145**, 373–80 (2015).
12. Day, R. E. *et al.* Human aquaporins: Regulators of transcellular water flow. *Biochim. Biophys. Acta - Gen. Subj.* **1840**, 1492–506 (2014).
13. Kedem, O. & Katchalsky, A. Thermodynamic analysis of the permeability of biological membranes to non-electrolytes. *Biochim. Biophys. Acta* **27**, 229–46 (1958).
14. Solenov, E. I., Baturina, G. S., Katkova, L. E. & Zarogiannis, S. G. Methods to Measure Water Permeability. *Adv. Exp. Med. Biol.* **969**, 263–276 (2017).
15. Ateshian, G. A., Morrison, B., Holmes, J. W. & Hung, C. T. Mechanics of cell growth. *Mech. Res. Commun.* **42**, 118–125 (2012).
16. Fletcher, D. A. & Mullins, R. D. Cell mechanics and the cytoskeleton. *Nature* **463**, 485–492 (2010).
17. Yancey, P. H. Organic osmolytes as compatible, metabolic and counteracting cytoprotectants in high osmolarity and other stresses. *J. Exp. Biol.* **208**, 2819–2830 (2005).

18. Deng, Y., Sun, M. & Shaevitz, J. W. Direct measurement of cell wall stress stiffening and turgor pressure in live bacterial cells. *Phys. Rev. Lett.* **107**, (2011).
19. Nezhad, A. S., Naghavi, M., Packirisamy, M., Bhat, R. & Geitmann, A. Quantification of the Young's modulus of the primary plant cell wall using Bending-Lab-On-Chip (BLOC). *Lab Chip* **13**, 2599–608 (2013).
20. Ponder, E. The measurement of red-cell volume. Conductivity measurements. *J. Physiol.* **85**, 439–49 (1935).
21. Essig, A. The 'Pump-Leak' Model and Exchange Diffusion. *Biophys. J.* **8**, 53–63 (1968).
22. Mori, Y. Mathematical properties of pump-leak models of cell volume control and electrolyte balance. *J. Math. Biol.* **65**, 875–918 (2012).
23. Feranchak, A. P. *et al.* p38 MAP kinase modulates liver cell volume through inhibition of membrane Na<sup>+</sup> permeability. *J. Clin. Invest.* **108**, 1495–1504 (2001).
24. Sinha, B. *et al.* Cells respond to mechanical stress by rapid disassembly of caveolae. *Cell* **144**, 402–13 (2011).
25. Groulx, N., Boudreault, F., Orlov, S. N. & Grygorczyk, R. Membrane reserves and hypotonic cell swelling. *J. Membr. Biol.* **214**, 43–56 (2006).
26. Hui, T. H. *et al.* Volumetric deformation of live cells induced by pressure-activated cross-membrane ion transport. *Phys. Rev. Lett.* **113**, (2014).
27. Zlotek-Zlotkiewicz, E., Monnier, S., Cappello, G., Le Berre, M. & Piel, M. Optical volume and mass measurements show that mammalian cells swell during mitosis. *J. Cell Biol.* **211**, 765–74 (2015).
28. Son, S. *et al.* Resonant microchannel volume and mass measurements show that suspended cells swell during mitosis. *J. Cell Biol.* **211**, 757–63 (2015).
29. Potočar, U. *et al.* Adipose-derived stem cells respond to increased osmolarities. *PLoS One* **11**, e0163870 (2016).
30. Hoffmann, E. K., Lambert, I. H. & Pedersen, S. F. Physiology of cell volume regulation in vertebrates. *Physiol. Rev.* **89**, 193–277 (2009).
31. Jiang, H. & Sun, S. X. Cellular pressure and volume regulation and implications for cell mechanics. *Biophys. J.* **105**, 609–19 (2013).
32. Haswell, E. S., Phillips, R. & Rees, D. C. Mechanosensitive channels: what can they do and how do they do it? *Structure* **19**, 1356–69 (2011).
33. Yang, N. J. & Hinner, M. J. Getting across the cell membrane: An overview for small molecules, peptides, and proteins. *Methods Mol. Biol.* **1266**, 29–53 (2015).
34. Hui, T. H. *et al.* Regulating the Membrane Transport Activity and Death of Cells via Electroosmotic Manipulation. *Biophys. J.* **110**, 2769–2778 (2016).
35. Roudaut, Y. *et al.* Touch sense: functional organization and molecular determinants of mechanosensitive receptors. *Channels (Austin)*. **6**, 234–45 (2012).
36. Wu, J., Lewis, A. H. & Grandl, J. Touch, Tension, and Transduction – The Function and Regulation of Piezo Ion Channels. *Trends Biochem. Sci.* **42**, 57–71 (2017).
37. Martinac, B. The ion channels to cytoskeleton connection as potential mechanism of

- mechanosensitivity. *Biochim. Biophys. Acta - Biomembr.* **1838**, 682–91 (2014).
38. Syeda, R. *et al.* LRRC8 Proteins Form Volume-Regulated Anion Channels that Sense Ionic Strength. *Cell* **164**, 499–511 (2016).
  39. Sachs, F. Stretch-activated ion channels: what are they? *Physiol.* **25**, 50–56 (2010).
  40. Han, F., Tucker, A. L., Lingrel, J. B., Despa, S. & Bers, D. M. Extracellular potassium dependence of the Na<sup>+</sup>-K<sup>+</sup>-ATPase in cardiac myocytes: isoform specificity and effect of phospholemman. *Am J Physiol Cell Physiol* **297**, 699–705 (2009).
  41. Burg, M. B., Ferraris, J. D. & Dmitrieva, N. I. Cellular response to hyperosmotic stresses. *Physiol. Rev.* **87**, 1441–74 (2007).
  42. Sands, Z., Grottesi, A. & Sansom, M. S. P. Voltage-gated ion channels. *Curr. Biol.* **15**, R44-7 (2005).
  43. Lloyd, A. C. The regulation of cell size. *Cell* **154**, 1194–205 (2013).
  44. Caron, A., Richard, D. & Laplante, M. The Roles of mTOR Complexes in Lipid Metabolism. *Annu. Rev. Nutr.* **35**, 321–348 (2015).
  45. Adhikary, S. & Eilers, M. Transcriptional regulation and transformation by Myc proteins. *Nat. Rev. Mol. Cell Biol.* **6**, 635–45 (2005).
  46. Son, S. *et al.* Direct observation of mammalian cell growth and size regulation. *Nat. Methods* **9**, 910–2 (2012).
  47. Cadart, C. *et al.* Size control in mammalian cells involves modulation of both growth rate and cell cycle duration. *Nat. Commun.* **9**, 3275 (2018).
  48. Godin, M. *et al.* Using buoyant mass to measure the growth of single cells. *Nat. Methods* **7**, 387–90 (2010).
  49. Osella, M., Nugent, E. & Cosentino Lagomarsino, M. Concerted control of Escherichia coli cell division. *Proc. Natl. Acad. Sci. U. S. A.* **111**, 3431–5 (2014).
  50. Taheri-Araghi, S. *et al.* Cell-Size Control and Homeostasis in Bacteria. *Curr. Biol.* **25**, 385–391 (2015).
  51. Reshes, G., Vanounou, S., Fishov, I. & Feingold, M. Cell Shape Dynamics in Escherichia coli. *Biophys. J.* **94**, 251–264 (2008).
  52. Nordholt, N., van Heerden, J. H. & Bruggeman, F. J. Integrated biphasic growth rate, gene expression, and cell-size homeostasis behaviour of single B. subtilis cells. *bioRxiv* 510925 (2019).
  53. Ferrezuelo, F. *et al.* The critical size is set at a single-cell level by growth rate to attain homeostasis and adaptation. *Nat. Commun.* **3**, 1012 (2012).
  54. Goranov, A. I. *et al.* The rate of cell growth is governed by cell cycle stage. *Genes Dev.* **23**, 1408–1422 (2009).
  55. Horváth, A., Rácz-Mónus, A., Buchwald, P. & Sveczer, Á. Cell length growth in fission yeast: An analysis of its bilinear character and the nature of its rate change transition. *FEMS Yeast Res.* **13**, 635–649 (2013).
  56. Kafri, R. *et al.* Dynamics extracted from fixed cells reveal feedback linking cell growth to cell cycle. *Nature* **494**, 480–483 (2013).

57. Sung, Y. *et al.* Size homeostasis in adherent cells studied by synthetic phase microscopy. *Proc. Natl. Acad. Sci. U. S. A.* **110**, 16687–92 (2013).
58. Mir, M. *et al.* Optical measurement of cycle-dependent cell growth. *Proc. Natl. Acad. Sci. U. S. A.* **108**, 13124–9 (2011).
59. Conlon, I. & Raff, M. Differences in the way a mammalian cell and yeast cells coordinate cell growth and cell-cycle progression. *J. Biol.* **2**, 7 (2003).
60. Mitchison, J. M. & Nurse, P. Growth in cell length in the fission yeast *Schizosaccharomyces pombe*. *J. Cell Sci.* **75**, (1985).
61. Baumgärtner, S. & Tolić-Nørrelykke, I. M. Growth pattern of single fission yeast cells is bilinear and depends on temperature and DNA synthesis. *Biophys. J.* **96**, 4336–4347 (2009).
62. Goranov, A. I. & Amon, A. Growth and division-not a one-way road. *Curr. Opin. Cell Biol.* **22**, 795–800 (2010).
63. Mitchison, J. M. Growth During the Cell Cycle. *Int. Rev. Cytol.* **226**, 165–258 (2003).
64. Glazier, D. Metabolic Scaling in Complex Living Systems. *Systems* **2**, 451–540 (2014).
65. Miettinen, T. P. & Bjorklund, M. Cellular Allometry of Mitochondrial Functionality Establishes the Optimal Cell Size. *Dev. Cell* **39**, 370–382 (2016).
66. Kafri, M. *et al.* The Cost of Protein Production. *Cell Rep.* **14**, 22–31 (2016).
67. Lin, J. & Amir, A. Homeostasis of protein and mRNA concentrations in growing cells. *Nat. Commun.* **9**, (2018).
68. Di Talia, S., Skotheim, J. M., Bean, J. M., Siggia, E. D. & Cross, F. R. The effects of molecular noise and size control on variability in the budding yeast cell cycle. *Nature* **448**, 947–51 (2007).
69. Schmoller, K. M. & Skotheim, J. M. The Biosynthetic Basis of Cell Size Control. *Trends Cell Biol.* **25**, 793–802 (2015).
70. Facchetti, G., Chang, F. & Howard, M. Controlling cell size through sizer mechanisms. *Curr. Opin. Syst. Biol.* **5**, 86–92 (2017).
71. Chandler-Brown, D., Schmoller, K. M., Winetraub, Y. & Skotheim, J. M. The Adder Phenomenon Emerges from Independent Control of Pre- and Post- Start Phases of the Budding Yeast Cell Cycle. *Curr. Biol.* **27**, 2774-2783.e3 (2017).
72. Dolznig, H., Grebien, F., Sauer, T., Beug, H. & Müllner, E. W. Evidence for a size-sensing mechanism in animal cells. *Nat. Cell Biol.* **6**, 899–905 (2004).
73. Liu, S. *et al.* Size uniformity of animal cells is actively maintained by a p38 MAPK-dependent regulation of G1-length. *Elife* **7**, (2018).
74. Varsano, G. *et al.* Probing Mammalian Cell Size Homeostasis by Article Probing Mammalian Cell Size Homeostasis by Channel-Assisted Cell Reshaping. *CellReports* **20**, 397–410 (2017).
75. Facchetti, G., Knapp, B., Flor-Parra, I., Chang, F. & Correspondence, M. H. Reprogramming Cdr2-Dependent Geometry-Based Cell Size Control in Fission Yeast. *Curr. Biol.* **29**, 1–9 (2018).
76. Garmendia-Torres, C., Tassy, O., Matifas, A., Molina, N. & Charvin, G. Multiple inputs ensure yeast cell size homeostasis during cell cycle progression. *Elife* **7**, 1–27 (2018).
77. Jonas, F., Soifer, I. & Barkai, N. A Visual Framework for Classifying Determinants of Cell Size.

*Cell Rep.* **25**, 3519–3529.e2 (2018).

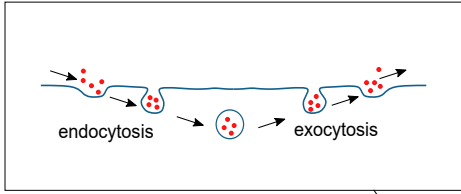
78. Fantès, P. A., Grant, W. D., Pritchard, R. H., Sudbery, P. E. & Wheals, A. E. The regulation of cell size and the control of mitosis. *J Theor Biol* **50**, 213–244 (1975).
79. Soifer, I., Robert, L. & Amir, A. Single-cell analysis of growth in budding yeast and bacteria reveals a common size regulation strategy. *Curr. Biol.* **26**, 356–361 (2016).
80. Schmoller, K. ., Turner, J. J., Kõivomägi, M. & Skotheim, J. M. Dilution of the cell cycle inhibitor Whi5 controls budding yeast cell size. *Nature* **526**, 268–272 (2015).
81. Zatulovskiy, E., Berenson, D. F., Topacio, B. R. & Skotheim, J. M. Cell growth dilutes the cell cycle inhibitor Rb to trigger cell division. *bioRxiv* 470013 (2018).
82. Sompayrac & Maaloe, O. Autorepressor Model for Control of DNA Replication. *Nat. new Biol.* **241**, (1973).
83. Harris, L. K. & Theriot, J. A. Relative rates of surface and volume synthesis set bacterial cell size. *Cell* **165**, 1479–1492 (2016).
84. Zielke, N. *et al.* Control of *Drosophila* endocycles by E2F and CRL4CDT2. *Nature* **480**, 123–127 (2011).
85. Heldt, F. S., Lunstone, R., Tyson, J. J. & Novák, B. Dilution and titration of cell-cycle regulators may control cell size in budding yeast. *PLoS Comput. Biol.* **14**, (2018).
86. Osella, M., Tans, S. J. & Cosentino Lagomarsino, M. Step by Step, Cell by Cell: Quantification of the Bacterial Cell Cycle. *Trends Microbiol.* **25**, 250–256 (2017).
87. Tzur, A., Kafri, R., Lebleu, V. S., Lahav, G. & Kirschner, M. W. Cell growth and size homeostasis in proliferating animal cells. *Science* **325**, 167–71 (2009).
88. Park, K. *et al.* Measurement of adherent cell mass and growth. *Proc. Natl. Acad. Sci. U. S. A.* **107**, 20691–6 (2010).
89. Ginzberg, M. B. *et al.* Cell size sensing in animal cells coordinates anabolic growth rates and cell cycle progression to maintain cell size uniformity. *Elife* **7**, e26947 (2018).
90. Amir, A. Cell Size Regulation in Bacteria. *Phys. Rev. Lett.* **112**, 208102 (2014).
91. Grilli, J., Osella, M., Kennard, A. S. & Lagomarsino, M. C. Relevant parameters in models of cell division control. *Phys. Rev. E - Stat. Nonlinear, Soft Matter Phys.* **032411**, (2017).
92. Kennard, A. S. *et al.* Individuality and universality in the growth-division laws of single *E. Coli* cells. *Phys. Rev. E - Stat. Nonlinear, Soft Matter Phys.* **93**, 1–18 (2016).
93. Bassetti, F., Epifani, I. & Ladelli, L. Cox Markov models for estimating single cell growth. *Electron. J. Stat.* **11**, 2931–2977 (2017).
94. Grilli, J., Cadart, C., Micali, G., Osella, M. & Cosentino Lagomarsino, M. The Empirical Fluctuation Pattern of *E. coli* Division Control. *Front. Microbiol.* **9**, 1–10 (2018).
95. Micali, G., Grilli, J., Marchi, J., Osella, M. & Cosentino Lagomarsino, M. Dissecting the Control Mechanisms for DNA Replication and Cell Division in *E. coli*. *Cell Rep.* **25**, 761–771.e4 (2018).
96. Martínez-Martín, D. *et al.* Inertial picobalance reveals fast mass fluctuations in mammalian cells. *Nature* **550**, 500–505 (2017).
97. Dolfi, S. C. *et al.* The metabolic demands of cancer cells are coupled to their size and protein synthesis rates. *Cancer Metab.* **1**, 20 (2013).

98. Marguerat, S. & Bähler, J. Coordinating genome expression with cell size. *Trends Genet.* **28**, 560–565 (2012).
99. Blackiston, D. J., McLaughlin, K. A. & Levin, M. Bioelectric controls of cell proliferation: ion channels, membrane voltage and the cell cycle. *Cell Cycle* **8**, 3527–36 (2009).
100. Rojas, E., Theriot, J. a & Huang, K. C. Response of Escherichia coli growth rate to osmotic shock. *Proc. Natl. Acad. Sci. U. S. A.* **111**, 7807–12 (2014).
101. Pilizota, T. & Shaevitz, J. W. Fast, multiphase volume adaptation to hyperosmotic shock by escherichia coli. *PLoS One* **7**, e35205 (2012).
102. de Nadal, E., Ammerer, G. & Posas, F. Controlling gene expression in response to stress. *Nat. Rev. Genet.* **12**, 833–45 (2011).
103. Geijer, C. *et al.* Initiation of the transcriptional response to hyperosmotic shock correlates with the potential for volume recovery. *FEBS J.* **280**, 3854–67. (2013).
104. Burg, M. B. & Garcia-Perez, A. How tonicity regulates gene expression. *J. Am. Soc. Nephrol.* **3**, 121–7 (1992).
105. Stoll, B., Gerok, W., Langt, F. & Haussinger, D. Liver cell volume and protein synthesis. *Biochem. J* **287**, 217–222 (1992).
106. Sukenik, S., Ren, P. & Gruebele, M. Weak protein–protein interactions in live cells are quantified by cell-volume modulation. *Proc. Natl. Acad. Sci.* **114**, 6776–6781 (2017).
107. Klumpp, S., Scott, M., Pedersen, S. & Hwa, T. Molecular crowding limits translation and cell growth. *Proc. Natl. Acad. Sci. U. S. A.* **110**, 16754–9 (2013).
108. Dill, K. A., Ghosh, K. & Schmit, J. D. Physical limits of cells and proteomes. *Proc. Natl. Acad. Sci. U. S. A.* **108**, 17876–82 (2011).
109. Bryan, A. K. *et al.* Measuring single cell mass, volume, and density with dual suspended microchannel resonators. *Lab Chip* **14**, 569–76 (2014).
110. Rojas, E. R. & Huang, K. C. Regulation of microbial growth by turgor pressure. *Current Opinion in Microbiology* (2018). doi:10.1016/j.mib.2017.10.015
111. Diz-Muñoz, A. *et al.* Membrane Tension Acts Through PLD2 and mTORC2 to Limit Actin Network Assembly During Neutrophil Migration. *PLOS Biol.* **14**, e1002474 (2016).
112. Rojas, E. R., Huang, K. C. & Theriot, J. A. Homeostatic Cell Growth Is Accomplished Mechanically through Membrane Tension Inhibition of Cell-Wall Synthesis. *Cell Syst.* **5**, 578–590 (2017).
113. Cermak, N. *et al.* High-throughput measurement of single-cell growth rates using serial microfluidic mass sensor arrays. *Nat Biotech* **34**, 1052–1059 (2016).
114. Kimmerling, R. J. *et al.* Linking single-cell measurements of mass, growth rate, and gene expression. *Genome Biol.* **19**, 207 (2018).
115. Kesavan, S. V. *et al.* High-throughput monitoring of major cell functions by means of lensfree video microscopy. *Sci. Rep.* **4**, 5942 (2014).
116. Mir, M., Bergamaschi, A., Katzenellenbogen, B. S. & Popescu, G. Highly sensitive quantitative imaging for monitoring single cancer cell growth kinetics and drug response. *PLoS One* **9**, e89000 (2014).

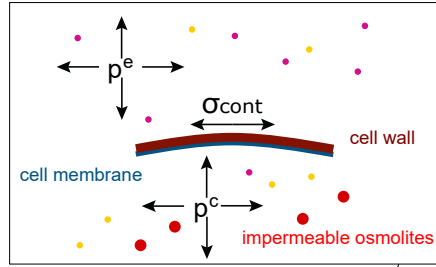
117. Fernandez-Fernandez, J. M., Nobles, M., Currid, A., Vazquez, E. & Valverde, M. A. Maxi K<sup>+</sup> channel mediates regulatory volume decrease response in a human bronchial epithelial cell line. *AJP Cell Physiol.* **283**, C1705–C1714 (2002).
118. Mitchison, J. M., Svecizer, A. & Novak, B. Length growth in fission yeast: is growth exponential? - No. *Microbiology* **144**, 265–266 (1998).
119. Ping Ting-Beall, B. H., Needham, D. & Hochmuth, R. M. Volume and Osmotic Properties of Human Neutrophils. *Blood.* **81**, 2774–2780 (1993).
120. Son, S. *et al.* Cooperative nutrient accumulation sustains growth of mammalian cells. *Sci. Rep.* **5**, (2015).
121. Sybren Ruurds de Groot & Mazur, P. *Non-Equilibrium Thermodynamics*. (North-Holland, 1962).
122. Prost, J., Jülicher, F. & Joanny, J. F. Active gel physics. *Nat. Phys.* **11**, 111–117 (2015).

**Mis en forme :** Couleur de police :  
Texte 1, Anglais (États Unis)

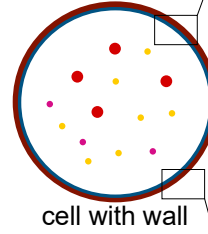
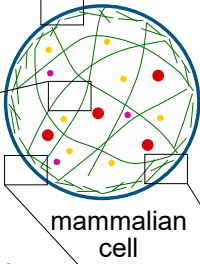
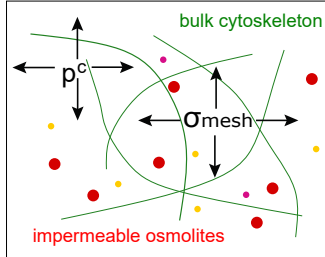
membrane turnover



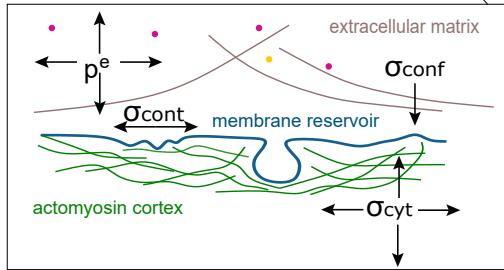
force balance on the wall



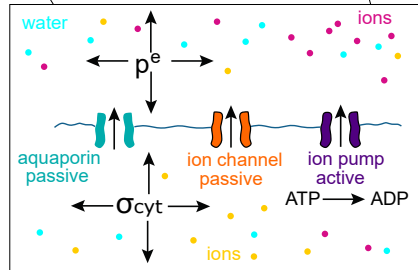
bulk



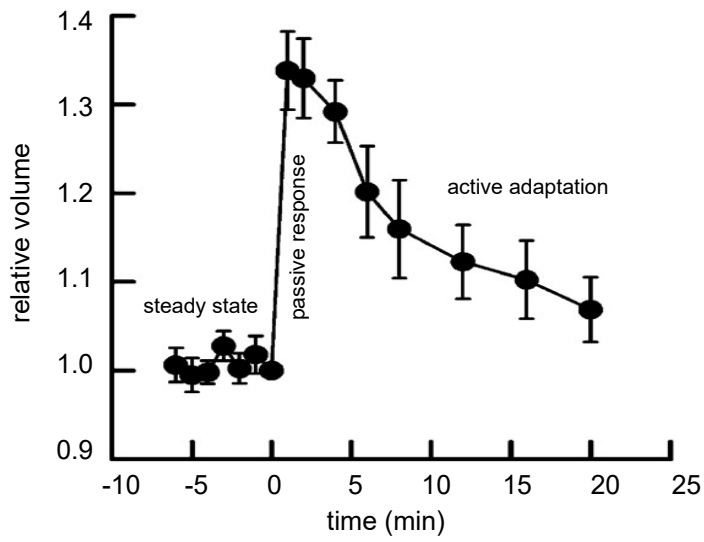
force balance on the membrane



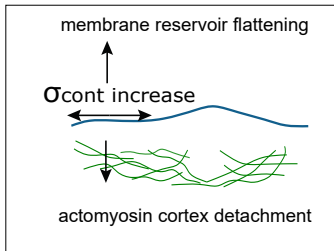
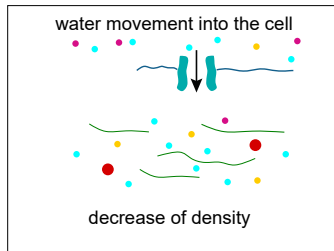
osmotic balance



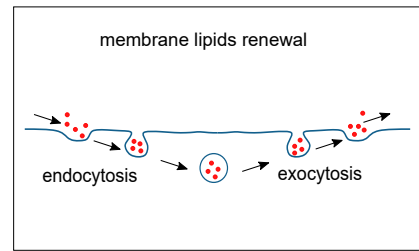
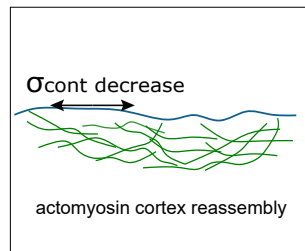
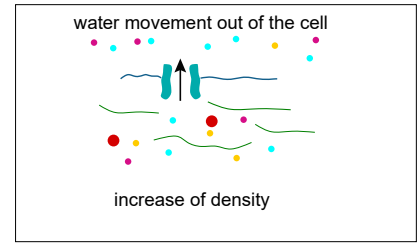
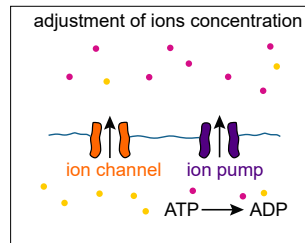
a

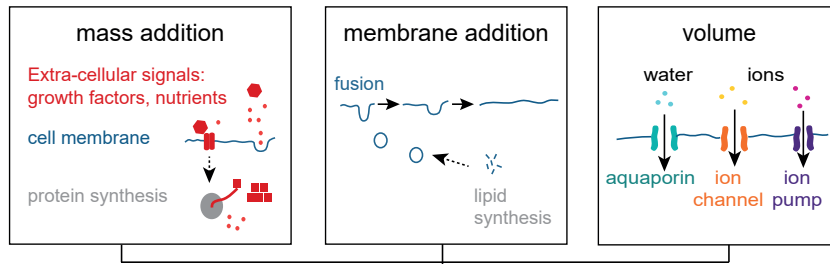
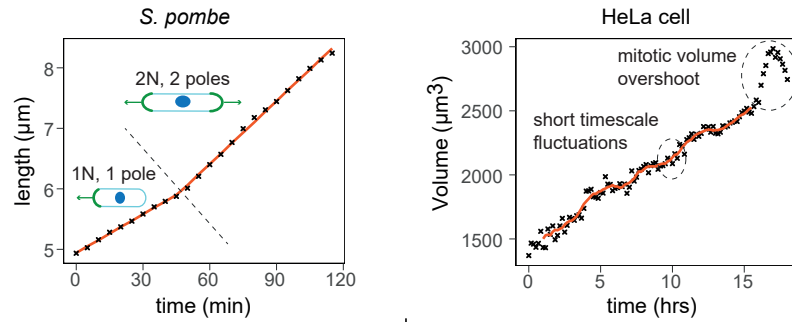
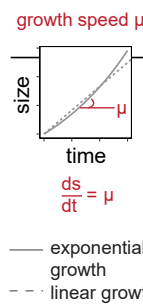
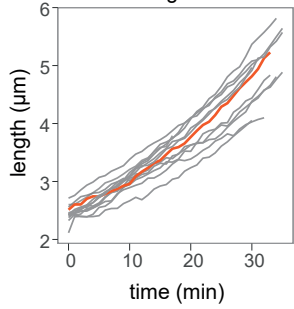
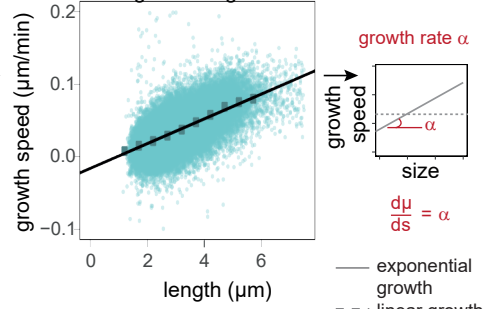
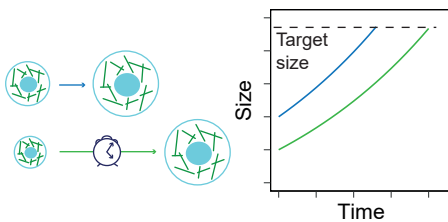
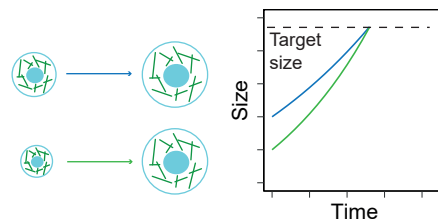


**b Fast passive response, swelling**

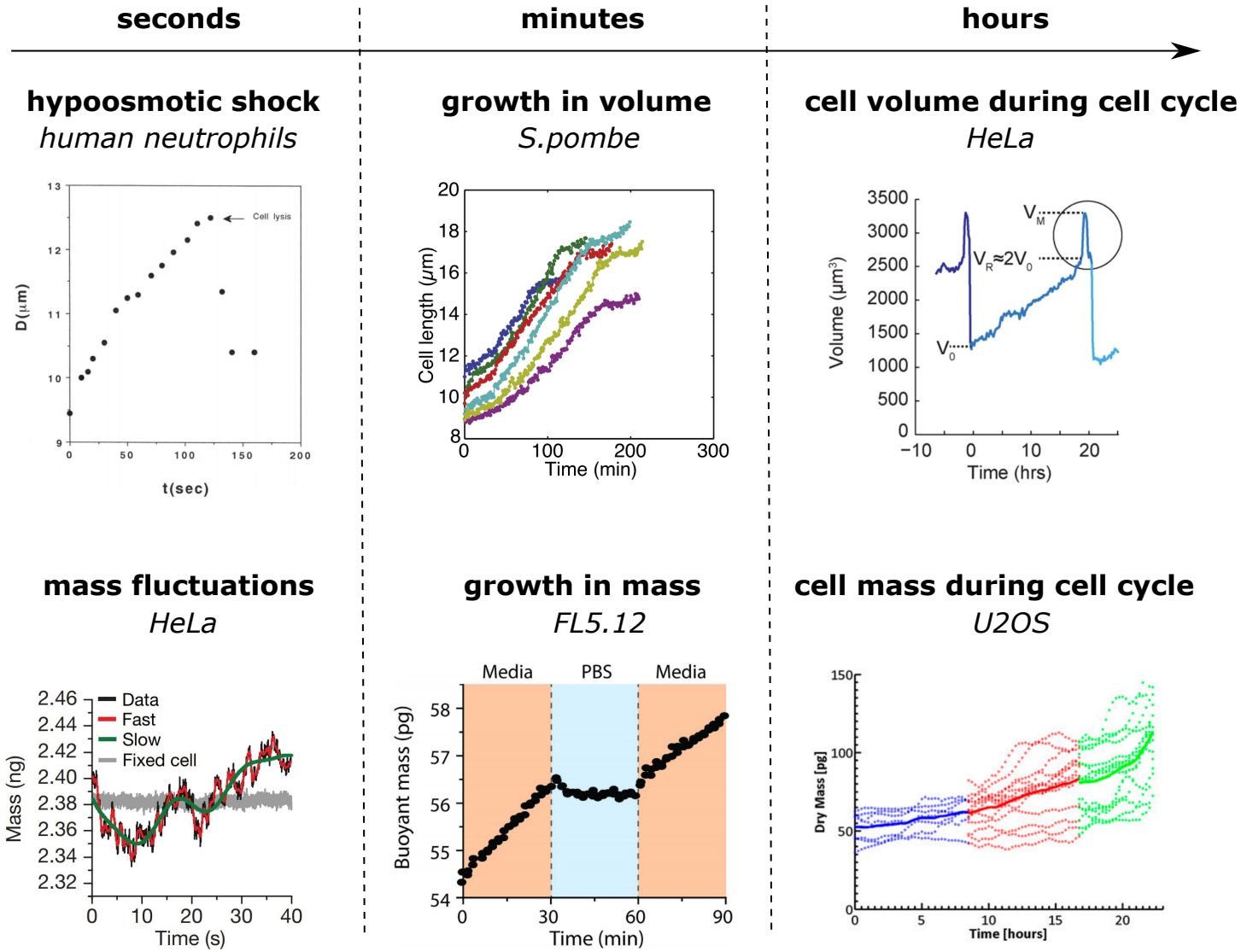


**c Active adaptation, RVD**



**a****Mechanisms of growth****b****Single cell growth****Average growth behaviour****c*****E. coli*: single cell curves****d*****E. coli*: averages of single cell curves****Coupling of growth with cell cycle progression****e****Modulation of division rate****f****Modulation of growth rate****Size homeostasis**

a



b

